Letter

Effects of Single α-to-β Residue Replacements on Recognition of an Extended Segment in a Viral Fusion Protein

Victor K. Outlaw, Dale F. Kreitler, Debora Stelitano, Matteo Porotto,* Anne Moscona,* and Samuel H. Gellman*

Cite This: https://dx.doi.org/10.1021/acsinfecdis.0c00385

Read Online

ACCESS | Metrics & More | Article Recommendations | Supporting Information

ABSTRACT: Partial replacement of α-amino acid residues with β-amino acid residues has been established as a strategy for preserving target-engagement by helix-forming polypeptides while altering other properties. The impact of β-residue incorporation within polypeptides that adopt less regular conformations, however, has received less attention. The C-terminal heptad repeat (HRC) domains of fusion glycoproteins from pathogenic paramyxoviruses contain a segment that must adopt an extended conformation in order to coassemble with the N-terminal heptad repeat (HRN) domain in the postfusion state and drive a merger of the viral envelope with a target cell membrane. Here, we examine the impact of single α-to-β substitutions within this extended N-terminal segment of an engineered HRC peptide designated VIQKI. Stabilities of hexameric coassemblies formed with the native human parainfluenza virus 3 (HPIV3) HRN have been evaluated, the structures of five coassemblies have been determined, and antiviral efficacies have been measured. Many sites within the extended segment show functional tolerance of α-to-β substitution. These results offer a basis for future development of paramyxovirus infection inhibitors with novel biological activity profiles, possibly including resistance to proteolysis.

KEYWORDS: α/β-peptide, β-amino acid, HPIV3, entry inhibitor, fusion glycoprotein, viral entry
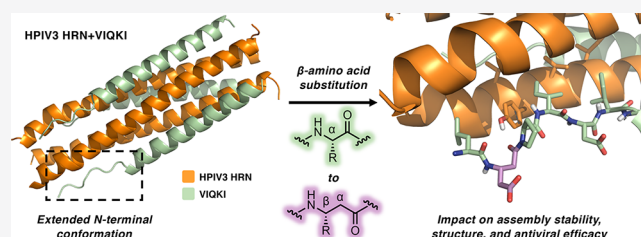
The disruption of interactions within or between proteins is an attractive basis for drug design. This strategy requires molecules that can engage large surfaces on target proteins, a goal that is generally difficult to achieve with small molecules (MW < 1000).[1−3] Clinically useful inhibitors of pathogenic protein−protein interactions are typically engineered proteins or large peptides. Antibodies and other large proteins are expensive to produce.[4] Smaller polypeptides offer the advantage of chemical synthesis but suffer from rapid degradation by endogenous proteases.[1−3] One strategy for retaining the benefits of polypeptides while minimizing proteolytic susceptibility is to incorporate non-natural subunits into the peptidic backbone.[5−12] The challenge inherent in this approach is to introduce a sufficient number and distribution of backbone modifications to hinder protease action without loss of target protein engagement. We have shown that the recognition properties of an α-helix can be retained after periodic replacement of α-amino acid residues with β-residues.[13−22] The resulting "α/β-peptides" adopt an α-helix-like conformation but resist enzymatic degradation. Less is known about the impact of β-residue incorporation in nonhelical segments.

Paramyxoviruses, such as parainfluenza, measles, Nipah, and Hendra viruses, are negative-strand RNA viruses that negatively impact global human health. Here, we describe fundamental studies of α-to-β modifications in the context of an extended segment that plays a critical role in a paramyxovirus infection mechanism. We focus on an eight-residue portion of the fusion (F) glycoprotein of human parainfluenza virus 3 (HPIV3). The F protein orchestrates fusion of the HPIV3 envelope and the outer membrane of a target cell. This process involves a complex set of structural transitions within an F trimer that ultimately leads to the formation of a "six-helix bundle" (6HB) assembly between N-terminal heptad repeat (HRN) and C-terminal heptad repeat (HRC) domains of F.[23−25] In the postfusion 6HB state, the N-terminal portion of the HRC domain (residues 449−456) adopts an extended conformation, while the majority of the HRC domain residues (457−484) form an α-helix (Figure 1A).[26]

The few previous evaluations of α-to-β modification in extended peptide ligands had variable outcomes. For example, three groups have explored systematic "β-scans" of short peptide antigens (8 or 9 residues) that bind to class I major histocompatibility complexes (MHC I).[27−29] In each system,
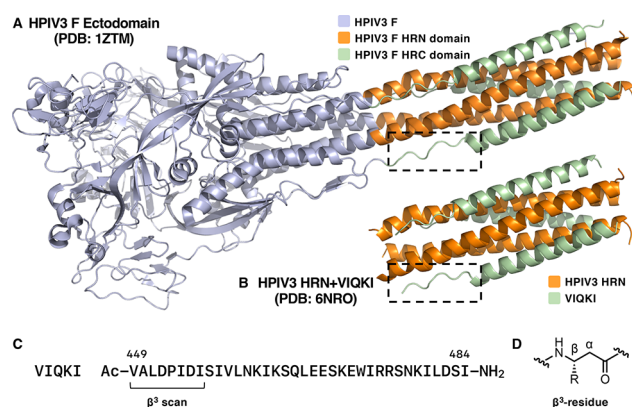
Figure 1. (A) HPIV3 F ectodomain in postfusion conformation (PDB 1ZTM), (B) VIQKI coassembled with HPIV3-HRN (PDB 6NRO), (C) sequence of VIQKI, and (D) structure of a β^3-residue.

MHC binding was retained for β-substitution at some positions, but most of the resulting peptide−MHC complexes were not effective in stimulating T cells that respond to the natural antigen. A subsequent study found greater functional tolerance of single α-to-β replacements in a 17-mer antigen that binds to a class II MHC.[30] A systematic α-to-β analogue series was recently reported for a 10-residue phosphopeptide that binds in an extended conformation to 14−3−3 proteins.[31] β-Substitution near either end caused modest declines in affinity (~10-fold), but more severe losses in affinity were observed for substitutions closer to the center of the peptide.

On the basis of these precedents, it was not clear whether α-to-β substitutions would be structurally or functionally tolerated within the extended portion of an HPIV3 inhibitor. We were motivated to proceed, however, by two considerations. First, peptide binding to an MHC or a 14−3−3 protein involves multiple H-bonds between the backbone of the peptide ligand and the protein partner. In contrast, there are relatively few H-bonds between the extended segment of the HPIV3 HRC domain and the HRN trimer core in the postfusion 6HB state of F. Second, coronaviruses (CoVs) feature even longer extended segments within the postfusion HRC domains of their fusion glycoproteins (S) than do paramyxoviruses, but the backbones of these extended CoV segments form relatively few H-bonds with the HRN trimer core.[32−34] α-to-β replacement seems likely to disrupt backbone H-bonding in an extended conformation; therefore, we predicted that this type of modification might be better tolerated in an extended segment of a viral fusion protein HRC domain than in other linear peptide epitopes.

METHODS

Our study began with a previously reported peptide derived from the HRC domain of HPIV3, designated VIQKI (Figure 1C), which blocks infection by both HPIV3 and respiratory syncytial virus (RSV).[35−37] These two viruses are leading causes of fatal lower respiratory infections in young children.[38−40] A crystal structure of VIQKI coassembled with HPIV3-HRN (Figure 1B) revealed a 6HB assembly similar to the HRC/HRN assembly in the postfusion conformation of the HPIV3 F protein (Figure 1A).[35] As expected, two distinct conformations were observed within the VIQKI peptide, an α-helix spanning residues corresponding to 457−484 of the F protein, and an extended conformation for residues corresponding to 449−456. Our studies focused on backbone

modifications in the extended portion of VIQKI (Figure 1, dashed boxes).

A set of VIQKI analogues was synthesized in which each of the eight N-terminal residues was replaced individually with the homologous β^3-amino acid residue (Figure 1D). Thus, each replacement preserved the side chain found in VIQKI but introduced an extra CH_2 unit into the backbone. The effect of each single α-to-β^3 substitution on assembly stability with HPIV3-HRN was examined using variable-temperature circular dichroism (VT-CD) spectroscopy. When combined with a 51-residue peptide corresponding to the HPIV3-HRN domain, each α/β-VIQKI variant formed a helical assembly, as detected by CD minima at 208 and 222 nm. Each assembly exhibited a cooperative thermal transition at 222 nm, which allowed us to determine apparent thermal denaturation ($T_{m,app}$) values, on the basis of the midpoint of each transition (Table 1). For each

Table 1. Apparent Thermal Denaturation Temperatures ($T_{m,app}$) of Coassemblies Formed between HPIV3-HRN +VIQKI β^3-Variant Pairs

peptide	$T_{m,app}$ (°C)[a]	$\Delta T_{m,app}$[b]
VIQKI	88.6 ± 0.4	
VIQKI-V449(β^3V)	89.0 ± 0.8	+0.4
VIQKI-A450(β^3A)	89.2 ± 1.0	+0.6
VIQKI-L451(β^3L)	88.7 ± 0.8	+0.1
VIQKI-D452(β^3D)	89.1 ± 0.4	+0.5
VIQKI-P453(β^3P)	86.1 ± 0.9	−2.5
VIQKI-I454(β^3I)	86.7 ± 1.0	−1.9
VIQKI-D455(β^3D)	81.5 ± 0.5	−7.1
VIQKI-I456(β^3I)	86.2 ± 1.1	−2.4

[a]1:1 mixture of inhibitor (50 μM) and HRN (50 μM) peptides. $T_{m,app}$ values were determined as mean values of three replicates ± standard deviation. [b]$\Delta T_{m,app}$ = $T_{m,app}$ (HPIV3-HRN+VIQKI β^3-variant) − $T_{m,app}$ (HPIV3-HRN+VIQKI).

α/β-VIQKI variant, a $\Delta T_{m,app}$ value was calculated on the basis of the comparison with $T_{m,app}$ for VIQKI itself [$\Delta T_{m,app}$ = $T_{m,app}$ (HPIV3-HRN+VIQKI β^3-variant) − $T_{m,app}$ (HPIV3-HRN+VIQKI)].

The VT-CD analysis revealed that most α-to-β replacements in the N-terminal region of VIQKI caused little or no change in $\Delta T_{m,app}$. Since omission of the three N-terminal residues (N449-L451) has little effect on HRC-HRN assembly stability,[35] it is perhaps not surprising that the β^3-residue was well tolerated at each of these positions. The D452-I456 segment, on the other hand, was shown by truncation studies to be crucial for assembly stability,[35] and it was therefore not expected that only one α-to-β replacement among these five residues, D455(β^3D), would be highly destabilizing.

To assess the functional impact of each single α-to-β substitution, we evaluated inhibitory activity toward HPIV3 infection using plaque reduction assays. Vero cell monolayers were infected with engineered recombinant HPIV3 that expresses green fluorescent protein (GFP) in the presence of various concentrations of each VIQKI variant, and the extent of infection was determined by quantification of fluorescence. The results are provided in two formats. Figure 2A shows the extent of inhibition of infection as a function of VIQKI variant concentration. Figure 2C shows the ratio of extent of inhibition for each variant relative to the inhibition for VIQKI itself at the experimental concentration closest to the IC_{50} of VIQKI (16 nM). Consistent with the VT-CD results, the functional data
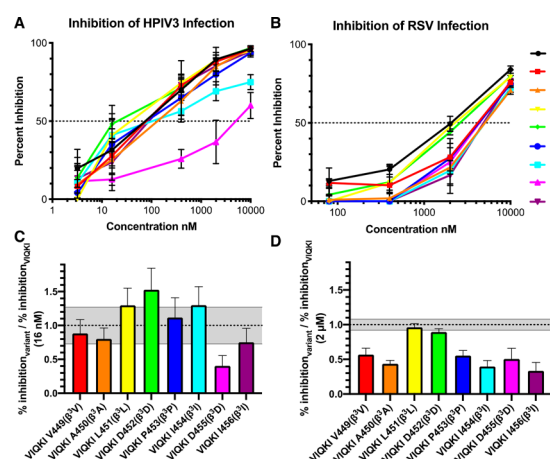
Figure 2. Antiviral efficacy of VIQKI β^3-variants against HPIV3 or RSV. Peptide activity against HPIV3 (left) or RSV (right) were determined by the plaque reduction assay in infected Vero cell monolayers. Data are shown as (A and B) percent inhibition of infection as a function of inhibitor concentration and (C and D) ratio of the percent inhibition of each β^3 variant with the percent inhibition of VIQKI, at 16 nM for HPIV3 or 2 μM for RSV (these concentrations are near the IC$_{50}$ of VIQKI for inhibiting each virus). Gray zones represent the standard deviation of the VIQKI control. Data are expressed as mean $\pm$ standard deviation (n = 3 separate experiments).

show that seven of the eight β-substituted peptides display substantial antiviral activity. Activity was lowest for the substitution that was most destabilizing to the HRC-HRN assembly, D455(β^3D).

The high sensitivity of D455 to β-residue replacement, in terms of both assembly stability and antiviral activity, was intriguing because of a critical role suggested by previous structural studies for the D455 side chain. The carboxylate of D455 in the postfusion 6HB form of the HPIV3 F protein engages in a H-bond with the backbone amide N−H of S457.[26] The same H-bond is seen in the cocrystal structure of VIQKI with the HPIV3 HRN domain.[35] This i, i + 2 interaction appears to serve as an N-terminal cap[41] for the α-helical secondary structure that starts at S457 and extends to the C-terminus.

To try to gain insight into the structural impact of the α-to-β substitutions, we cocrystallized five VIQKI variants with the HPIV3-HRN peptide, D452(β^3D), P453(β^3P), I454(β^3I), D455(β^3D), and I456(β^3I). Each structure was solved by molecular replacement using a search model based on the HPIV3-HRN+VIQKI structure (PDB 6NRO).[35] Chains A and B from 6NRO were truncated to include residues 153−173 (chain A) and 460−480 (chain B). All hydrogen atoms and side chains were removed prior to molecular replacement. Crystallographic models were refined to 1.70 Å [HPIV3-HRN +VIQKI-D452(β^3D), (PDB 6PZ6)]; 1.87 Å [HPIV3-HRN +VIQKI-P453(β^3P), (PDB 6PRL)]; 1.49 Å [HPIV3-HRN +VIQKI-I454(β^3I), (PDB 6VAS)]; 1.79 Å [HPIV3-HRN +VIQKI-D455(β^3D), (PDB 6PYQ)]; 2.17 Å [HPIV3-HRN +VIQKI-I456(β^3I), (PDB 6V3V)].

In each of the five new structures, the single β^3-residue substitution within the extended N-terminal segment did not affect the α-helical conformation of residues 457−484. However, the impact of α-to-β^3 substitution on the conformation of the N-terminal segment differed among the five variants (Figure 3).
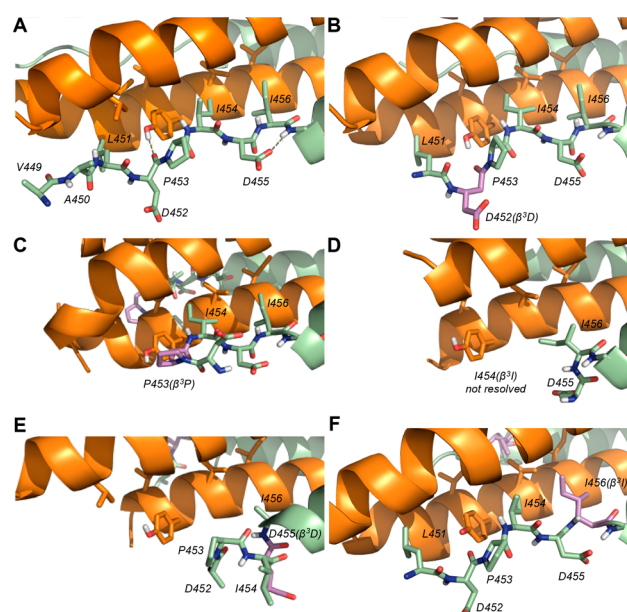

Figure 3. X-ray crystal structures of VIQKI and β^3-variants coassembled with HPIV3-HRN. (A) HPIV3-HRN+VIQKI, PDB: 6NRO; (B) HPIV3-HRN+VIQKI-D452(β^3D), PDB: 6PZ6; (C) HPIV3-HRN+VIQKI-P453(β^3P), PDB: 6PRL; (D) HPIV3-HRN +VIQKI-I454(β^3I), PDB: 6VAS; (E) HPIV3-HRN+VIQKI-D455-(β^3D), PDB: 6PYQ; (F) HPIV3-HRN+VIQKI-I456(β^3I), PDB: 6V3V. HPIV3-HRN (orange), VIQKI, and β^3-variants (green) with β^3-residues highlighted in violet.

In three of the five cocrystal structures, those containing P453(β^3P), I454(β^3I), or D455(β^3D) substitutions, the backbone modification resulted in a significant remodeling of the extended conformation in the N-terminal region relative to VIQKI. For VIQKI-P453(β^3P), contacts involving the I454 and I456 side chains and hydrophobic residues from the HPIV3-HRN trimer were retained, as was the helix capping interaction of D455. However, this substitution nucleated a hairpin turn that reoriented residues 449−452, with the loss of contacts observed between these residues in VIQKI and HPIV3-HRN (Figures 3C and 4B). Since previous work showed that contacts involving residues 449−451 do not significantly contribute to six-helix bundle stability,[35] this distortion may reflect the effects of packing with lattice neighbors. For VIQKI-I454(β^3I), only residues 455−484 could be resolved. No significant electron density was observed for the β^3I residue or residues 449−453.

In the coassembly of VIQKI-D455(β^3D) and HPIV3-HRN, residues 452−484 of the VIQKI variant were resolved. However, the transition from extended to α-helical conformation, which occurred at S457 in the HPIV3-HRN +VIQKI structure, was not observed for the D455(β^3D) variant. Instead, VIQKI-D455(β^3D) adopted a helical conformation from residue 453 to 484 (Figures 3E and 4C). We hypothesize that the additional backbone carbon atom between the carboxylate side chain of β^3D455 and the backbone amide N−H of S457 in this variant, relative to VIQKI itself, interferes with the helix-capping interaction involving the side chain of D455 in VIQKI. This conformational rearrangement in the N-terminal segment may explain the loss of 6HB stability (Table 1) and diminished antiviral activity (Figure 2) observed for VIQKI-D455(β^3D).
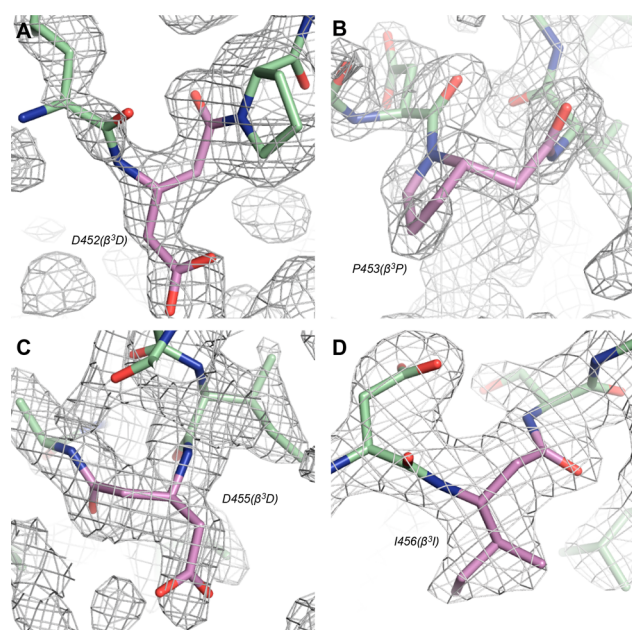
C

Figure 4. 2mFo-DFc weighted electron density maps for β^3-residues in (A) HPIV3-HRN+VIQKI-D452(β^3D), (B) HPIV3-HRN+VIQKI-P453(β^3P), (C) HPIV3-HRN+VIQKI-D455(β^3D), and (D) HPIV3-HRN+VIQKI-I456(β^3I). β^3-residues are shown in violet.

In the crystal structures of VIQKI-D452(β^3D) and VIQKI-I456(β^3I) coassembled with HPIV3-HRN, the extended conformation observed for VIQKI itself was retained (Figure 3B,F), although in both variants the two terminal residues, V449 and A450, could not be resolved. In both structures, key interactions between the N-terminal segment of the inhibitor and the HPIV3-HRN core were preserved. These interactions include contacts of side chains from L451, I454, and I456 (or β^3I456) with hydrophobic residues in the HRN trimer as well as H-bonds between the backbone carbonyl of D452 with the side chain hydroxyl of HRN residue Y178. The helix capping interaction was present in both of these VIQKI variants.

Although assessing activity of the β-substituted analogues of VIQKI toward RSV was tangential to the main goals of this work, we evaluated these peptides for the ability to inhibit RSV infection of Vero cells. Figure 2B,D shows that the effect of α-to-β substitutions on the efficacy against RSV was more pronounced than the effect on the efficacy against HPIV3. Most VIQKI variants were significantly less active relative to VIQKI itself. However, variants L451(β^3L) and D452(β^3D) seemed to match VIQKI in efficacy against RSV infection. The N-terminal segment of VIQKI adopts different conformations when coassembled with HPIV3-HRN vs RSV-HRN.[30] Residues P453–I456 are part of the extended segment in the assembly with HPIV3-HRN, but these residues have been incorporated into the α-helix in the assembly with RSV-HRN. It is noteworthy that only two variants, L451(β^3L) and D452(β^3D), maintained inhibition of infection by both viruses.

We have used a peptide that inhibits HPIV3 infection via a well-characterized mode of target engagement to explore the effects of replacing α-amino acid residues by homologous β^3-residues within a segment that is extended in the bioactive conformation. This modification preserves the side chain but alters the backbone via introduction of a CH_2 unit. On the basis of previous studies involving β-replacements in extended peptide ligands, it could not have been predicted that most

sites in the extended portion of the α-peptide inhibitor VIQKI would tolerate α-to-β^3 substitution while retaining the ability to inhibit HPIV3 infection. We hypothesize that the extended segments of viral HRC domains in the 6HB assemblies of postfusion forms may generally prove to be tolerant of backbone modifications because the backbone amide groups in these segments form few H-bonds with HRN domain trimers. This work offers a step toward development of protease-resistant dual HPIV3/RSV inhibitors that might address life-threatening childhood infections for which there are no current drugs. (We have not examined the effects of proteases on the β-substituted peptides discussed here, because with only one backbone modification, these 36-mers will undoubtedly be susceptible at most sites of potential cleavage.) In addition, given the presence of long extended segments in the postfusion HRC/HRN assemblies formed by coronavirus fusion glycoproteins,[32−34] these results encourage the application of the backbone modification strategy for inhibitor development directed toward these pathogens.

■ ASSOCIATED CONTENT

ⓢ Supporting Information

The Supporting Information is available free of charge at https://pubs.acs.org/doi/10.1021/acsinfecdis.0c00385.

> Synthetic procedures, MALDI-TOF MS analysis, UPLC purity analysis, circular dichroism spectra, thermal denaturation, crystal morphologies, and characterization data for all synthesized peptides as well as protocols for plaque reduction and thermal denaturation assays (PDF)

■ AUTHOR INFORMATION

Corresponding Authors

Samuel H. Gellman − *Department of Chemistry, University of Wisconsin, Madison, Wisconsin 53706, United States;* ⓞ orcid.org/0000-0001-5617-0058; Email: gellman@chem.wisc.edu

Anne Moscona − *Department of Pediatrics, Center for Host−Pathogen Interaction, Department of Microbiology & Immunology, and Department of Physiology & Cellular Biophysics, Columbia University Medical Center, New York, New York 10032, United States;* Email: am939@cumc.columbia.edu

Matteo Porotto − *Department of Pediatrics and Center for Host−Pathogen Interaction, Columbia University Medical Center, New York, New York 10032, United States; Department of Experimental Medicine, University of Campania "Luigi Vanvitelli", 81100 Caserta, Italy;* Email: mp3509@cumc.columbia.edu

Authors

Victor K. Outlaw − *Department of Chemistry, University of Wisconsin, Madison, Wisconsin 53706, United States;* ⓞ orcid.org/0000-0001-7054-4204

Dale F. Kreitler − *Department of Chemistry, University of Wisconsin, Madison, Wisconsin 53706, United States*

Debora Stelitano − *Department of Pediatrics and Center for Host−Pathogen Interaction, Columbia University Medical Center, New York, New York 10032, United States; Department of Experimental Medicine, University of Campania "Luigi Vanvitelli", 81100 Caserta, Italy*

Complete contact information is available at:

Notes

The authors declare no competing financial interest.

■ REFERENCES

(1) Fosgerau, K., and Hoffmann, T. (2015) Peptide Therapeutics: Current Status and Future Directions. *Drug Discovery Today 20* (1), 122−128.

(2) Lau, J. L., and Dunn, M. K. (2018) Therapeutic Peptides: Historical Perspectives, Current Development Trends, and Future Directions. *Bioorg. Med. Chem. 26* (10), 2700−2707.

(3) Henninot, A., Collins, J. C., and Nuss, J. M. (2018) The Current State of Peptide Drug Discovery: Back to the Future? *J. Med. Chem. 61* (4), 1382−1414.

(4) Elgundi, Z., Reslan, M., Cruz, E., Sifniotis, V., and Kayser, V. (2017) The State-of-Play and Future of Antibody Therapeutics. *Adv. Drug Delivery Rev. 122* (C), 2−19.

(5) Nowick, J. S., Lam, K. S., Khasanova, T. V., Kemnitzer, W. E., Maitra, S., Mee, H. T., and Liu, R. (2002) An Unnatural Amino Acid That Induces Beta-Sheet Folding and Interaction in Peptides. *J. Am. Chem. Soc. 124* (18), 4972−4973.

(6) Wang, D., Chen, K., Kulp, J. L., and Arora, P. S. (2006) Evaluation of Biologically Relevant Short Alpha-Helices Stabilized by a Main-Chain Hydrogen-Bond Surrogate. *J. Am. Chem. Soc. 128* (28), 9248−9256.

(7) Goodman, C. M., Choi, S., Shandler, S., and DeGrado, W. F. (2007) Foldamers as Versatile Frameworks for the Design and Evolution of Function. *Nat. Chem. Biol. 3* (5), 252−262.

(8) Henchey, L. K., Jochim, A. L., and Arora, P. S. (2008) Contemporary Strategies for the Stabilization of Peptides in the A-Helical Conformation. *Curr. Opin. Chem. Biol. 12* (6), 692−697.

(9) Azzarito, V., Long, K., Murphy, N. S., and Wilson, A. J. (2013) Inhibition of A-Helix-Mediated Protein−Protein Interactions Using Designed Molecules. *Nat. Chem. 5* (3), 161−173.

(10) Barnard, A., Long, K., Martin, H. L., Miles, J. A., Edwards, T. A., Tomlinson, D. C., Macdonald, A., and Wilson, A. J. (2015) Selective and Potent Proteomimetic Inhibitors of Intracellular Protein-Protein Interactions. *Angew. Chem., Int. Ed. 54* (10), 2960−2965.

(11) Wu, H., Qiao, Q., Teng, P., Hu, Y., Antoniadis, D., Zuo, X., and Cai, J. (2015) New Class of Heterogeneous Helical Peptidomimetics. *Org. Lett. 17* (14), 3524−3527.

(12) Bolarinwa, O., Zhang, M., Mulry, E., Lu, M., and Cai, J. (2018) Sulfono-γ-AA Modified Peptides That Inhibit HIV-1 Fusion. *Org. Biomol. Chem. 16* (42), 7878−7882.

(13) Horne, W. S., Johnson, L. M., Ketas, T. J., Klasse, P. J., Lu, M., Moore, J. P., and Gellman, S. H. (2009) Structural and Biological Mimicry of Protein Surface Recognition by Alpha/Beta-Peptide Foldamers. *Proc. Natl. Acad. Sci. U. S. A. 106* (35), 14751−14756.

(14) Johnson, L. M., Horne, W. S., and Gellman, S. H. (2011) Broad Distribution of Energetically Important Contacts Across an Extended Protein Interface. *J. Am. Chem. Soc. 133* (26), 10038−10041.

(15) Boersma, M. D., Haase, H. S., Peterson-Kaufman, K. J., Lee, E. F., Clarke, O. B., Colman, P. M., Smith, B. J., Horne, W. S., Fairlie, W. D., and Gellman, S. H. (2012) Evaluation of Diverse α/β-Backbone Patterns for Functional α-Helix Mimicry: Analogues of the Bim BH3 Domain. *J. Am. Chem. Soc. 134* (1), 315−323.

(16) Johnson, L. M., Mortenson, D. E., Yun, H. G., Horne, W. S., Ketas, T. J., Lu, M., Moore, J. P., and Gellman, S. H. (2012) Enhancement of α-Helix Mimicry by an α/β-Peptide Foldamer via Incorporation of a Dense Ionic Side-Chain Array. *J. Am. Chem. Soc. 134* (17), 7317−7320.

(17) Smith, B. J., Lee, E. F., Checco, J. W., Evangelista, M., Gellman, S. H., and Fairlie, W. D. (2013) Structure-Guided Rational Design of α/β-Peptide Foldamers with High Affinity for BCL-2 Family Prosurvival Proteins. *ChemBioChem 14* (13), 1564−1572.

(18) Cheloha, R. W., Maeda, A., Dean, T., Gardella, T. J., and Gellman, S. H. (2014) Backbone Modification of a Polypeptide Drug Alters Duration of Action in Vivo. *Nat. Biotechnol. 32* (7), 653−655.

(19) Johnson, L. M., Barrick, S., Hager, M. V., McFedries, A., Homan, E. A., Rabaglia, M. E., Keller, M. P., Attie, A. D., Saghatelian, A., Bisello, A., and Gellman, S. H. (2014) A Potent α/β-Peptide Analogue of GLP-1 with Prolonged Action in Vivo. *J. Am. Chem. Soc. 136* (37), 12848−12851.

(20) Checco, J. W., Kreitler, D. F., Thomas, N. C., Belair, D. G., Rettko, N. J., Murphy, W. L., Forest, K. T., and Gellman, S. H. (2015) Targeting Diverse Protein-Protein Interaction Interfaces with α/β-Peptides Derived From the Z-Domain Scaffold. *Proc. Natl. Acad. Sci. U. S. A. 112* (15), 4552−4557.

(21) Peterson-Kaufman, K. J., Haase, H. S., Boersma, M. D., Lee, E. F., Fairlie, W. D., and Gellman, S. H. (2015) Residue-Based Preorganization of BH3-Derived α/β-Peptides: Modulating Affinity, Selectivity and Proteolytic Susceptibility in α-Helix Mimics. *ACS Chem. Biol. 10* (7), 1667−1675.

(22) Olson, K. E., Kosloski-Bilek, L. M., Anderson, K. M., Diggs, B. J., Clark, B. E., Gledhill, J. M., Shandler, S. J., Mosley, R. L., and Gendelman, H. E. (2015) Selective VIP Receptor Agonists Facilitate Immune Transformation for Dopaminergic Neuroprotection in MPTP-Intoxicated Mice. *J. Neurosci. 35* (50), 16463−16478.

(23) Harrison, S. C. (2008) Viral Membrane Fusion. *Nat. Struct. Mol. Biol. 15* (7), 690−698.

(24) Chang, A., and Dutch, R. E. (2012) Paramyxovirus Fusion and Entry: Multiple Paths to a Common End. *Viruses 4* (12), 613−636.

(25) Kielian, M. (2014) Mechanisms of Virus Membrane Fusion Proteins. *Annu. Rev. Virol. 1* (1), 171−189.

(26) Yin, H.-S., Paterson, R. G., Wen, X., Lamb, R. A., and Jardetzky, T. S. (2005) Structure of the Uncleaved Ectodomain of the Paramyxovirus (hPIV3) Fusion Protein. *Proc. Natl. Acad. Sci. U. S. A. 102* (26), 9288−9293.

(27) Guichard, G., Zerbib, A., Le Gal, F. A., Hoebeke, J., Connan, F., Choppin, J., Briand, J. P., and Guillet, J. G. (2000) Melanoma peptide MART-1(27−35) analogues with enhanced binding capacity to the human class I histocompatibility molecule HLA-A2 by introduction of a β-amino acid residue: Implications for recognition by tumor-infiltrating lymphocytes. *J. Med. Chem. 43*, 3803−3808.

(28) Reinelt, S., Marti, M., Dedier, S., Reitinger, T., Folkers, G., de Castro, J. A. L., and Rognan, D. (2001) β-Amino acid scan of a Class I major histocompatibility complex-restricted alloreactive T-cell epitope. *J. Biol. Chem. 276*, 24525−24530.

(29) Webb, A. I., Dunstone, M. A., Williamson, N. A., Price, J. D., de Kauwe, A., Chen, W. S., Oakley, A., Perlmutter, P., McCluskey, J., Aguilar, M. I., Rossjohn, J., and Purcell, A. W. (2005) T cell determinants incorporating β-amino acid residues are protease resistant and remain immunogenic in vivo. *J. Immunol. 175*, 3810−3818.

(30) Cheloha, R. W., Woodham, A. W., Bousbaine, D., Wang, T., Liu, S., Sidney, J., Sette, A., Gellman, S. H., and Ploegh, H. L. (2019) Recognition of Class II MHC Peptide Ligands That Contain B-Amino Acids. *J. Immunol. 203* (6), 1619−1628.

(31) Andrei, S. A., Thijssen, V., Brunsveld, L., Ottmann, C., and Milroy, L.-G. (2019) A Study on the Effect of Synthetic α-to-β 3-

Amino Acid Mutations on the Binding of Phosphopeptides to 14−3-3 Proteins. *Chem. Commun.* 55 (98), 14809−14812.

(32) Duquerroy, S., Vigouroux, A., Rottier, P. J. M., Rey, F. A., and Jan Bosch, B. (2005) Central Ions and Lateral Asparagine/Glutamine Zippers Stabilize the Post-Fusion Hairpin Conformation of the SARS Coronavirus Spike Glycoprotein. *Virology* 335 (2), 276−285.

(33) Lu, L., Liu, Q., Zhu, Y., Chan, K.-H., Qin, L., Li, Y., Wang, Q., Chan, J. F.-W., Du, L., Yu, F., Ma, C., Ye, S., Yuen, K.-Y., Zhang, R., and Jiang, S. (2014) Structure-Based Discovery of Middle East Respiratory Syndrome Coronavirus Fusion Inhibitor. *Nat. Commun.* 5 (1), 3067.

(34) Xia, S., Yan, L., Xu, W., Agrawal, A. S., Algaissi, A., Tseng, C.-T. K., Wang, Q., Du, L., Tan, W., Wilson, I. A., Jiang, S., Yang, B., and Lu, L. (2019) A Pan-Coronavirus Fusion Inhibitor Targeting the HR1 Domain of Human Coronavirus Spike. *Sci. Adv.* 5 (4), eaav4580.

(35) Outlaw, V. K., Bottom-Tanzer, S., Kreitler, D. F., Gellman, S. H., Porotto, M., and Moscona, A. (2019) Dual Inhibition of Human Parainfluenza Type 3 and Respiratory Syncytial Virus Infectivity with a Single Agent. *J. Am. Chem. Soc.* 141 (32), 12648−12656.

(36) Outlaw, V. K., Lemke, J. T., Zhu, Y., Gellman, S. H., Porotto, M., and Moscona, A. (2020) Structure-Guided Improvement of a Dual HPIV3/RSV Fusion Inhibitor. *J. Am. Chem. Soc.* 142 (5), 2140−2144.

(37) Marcink, T. C., Yariv, E., Rybkina, K., Más, V., Bovier, F. T., des Georges, A., Greninger, A. L., Alabi, C. A., Porotto, M., Ben-Tal, N., and Moscona, A. (2020) Hijacking the Fusion Complex of Human Parainfluenza Virus as an Antiviral Strategy. *mBio* 11 (1), 1969−15.

(38) Nair, H., Nokes, D. J., Gessner, B. D., Dherani, M., Madhi, S. A., Singleton, R. J., O'Brien, K. L., Roca, A., Wright, P. F., Bruce, N., Chandran, A., Theodoratou, E., Sutanto, A., Sedyaningsih, E. R., Ngama, M., Munywoki, P. K., Kartasasmita, C., Simões, E. A., Rudan, I., Weber, M. W., and Campbell, H. (2010) Global Burden of Acute Lower Respiratory Infections Due to Respiratory Syncytial Virus in Young Children: a Systematic Review and Meta-Analysis. *Lancet* 375 (9725), 1545−1555.

(39) Englund, J. A., and Moscona, A. (2014) Paramyxoviruses: Parainfluenza viruses. In *Viral Infections of Humans* (Kaslow, R. A., Stanberry, L. R., and LeDuc, J. W., Eds.), pp 579−600, Springer, New York.

(40) Weinberg, G. A., Hall, C. B., Iwane, M. K., Poehling, K. A., Edwards, K. M., Griffin, M. R., Staat, M. A., Curns, A. T., Erdman, D. D., and Szilagyi, P. G. (2009) New Vaccine Surveillance Network. Parainfluenza Virus Infection of Young Children: Estimates of the Population-Based Burden of Hospitalization. *J. Pediatr.* 154 (5), 694−699.

(41) Serrano, L., and Fersht, A. R. (1989) Capping and A-Helix Stability. *Nature* 342 (6247), 296−299.